

Proceedings of the
MATERIALS PROCESSING SYMPOSIUM

ICALEO '83

November 14-17, 1983



77.9784
M 425

Proceedings of the
MATERIALS PROCESSING SYMPOSIUM

ICALEO 83

LIA VOLUME 38

EDITOR

Edward A Metzbow
Naval Research Laboratory
Washington, D C

Organized in Cooperation with the following Societies

The American Ceramic Society
The American Society of Laser Medicine and Surgery
The American Society of Metals
The American Welding Society
The High Temperature Society of Japan
The Inter-American Photochemical Society
The Materials Research Society
The Society for the Advancement of Material and Process Engineering
The Society of Automotive Engineers
The Society of Manufacturing Engineers
SPIE- The International Society for Optical Engineers
Verein Deutscher Ingenieure



Sponsored by:
THE LASER INSTITUTE OF AMERICA

Published by the LIA- Laser Institute of America
5151 Monroe Stree , Ste 118W
Toledo, OH 43623

175

8650175

2573/10
The papers appearing in this book comprise the proceedings of the meeting indicated on the cover and title page. They reflect the author's opinions and are published as received. Their inclusion in this publication does not necessarily constitute endorsement by the Laser Institute of America.

ISBN 0-912035-19-6

© 1984 Laser Institute of America
5151 Monroe St
Toledo, OH 43623

Individual readers of this publication and non-profit libraries acting for them are freely permitted to make fair use of the material in it, such as to copy an article for use in teaching or research. Permission is granted to quote excerpts from articles in this book in scientific or technical works with the customary acknowledgement of the source, including the author's name, the book name, LIA Volume number, page, and year. Reproduction of Figures and Tables is likewise permitted in other articles and books provided the same information is given and notification given to the LIA. LIA recognizes the right of the United States government to retain a nonexclusive, royalty-free license to use the author's copyrighted article for United States government purposes.

Program Committees

1. MEDICINE & BIOLOGY

Rocco Lobraico, M.D., Chairman
Ravenswood Hospital
Vernon Jobson, M.D.
Bowman Gray School of Medicine
Robert Ossoff, M.D.
Evanston, Illinois
Leonard Cerullo, M.D.
Northwestern University
Michael Burns, Ph.D.
University Cal. at Irvine

2. MATERIALS PROCESSING

Edward A. Metzbower, Chairman
Naval Res. Labs
Michael J. Bass
Univ. So. Calif.
Stephen M. Copley
Univ. So. Calif.
Marshall Jones
General Electric
Stanley L. Ream
Battelle Columbus Labs
Prof. William Steen
Imperial College

3. INSPECTION, MEASUREMENT & CONTROL

Warren H. Stevenson, Chairman
Purdue University
Jack Fleischer
Photon Tech.
Randall Schmitt
Western Electric
Dr. A. K. Bejczy
Jet Prop. Lab
Tom Stapleton
GM Tech Center

4. OPTICAL COMMUNICATIONS

Suzanne R. Nagel, Chairman
Bell Labs
J. Goell
Lightwave Tech
M. Hudson
Valtec Corp.
D. Jablonowski
Western Elec.
A. Glista
Naval Air Sys. Com.
J. Hsieh,
Lasertron, Inc.

5. INFORMATION PROCESSING & HOLOGRAPHY

Milton T. Chang, Chairman
Newport Rsh. Corp.
David Casasent, Co-chairman
Carnegie-Mellon Univ.

6. SCIENTIFIC APPLICATIONS OF LASERS

Robert O. Godwin, Co-chairman
Livermore National Lab
Jack P. Aldridge, Co-chairman
Los Alamos National Lab
Wayne Johnson
Sandia Nat'l. Lab
Clyde Layne
Sandia Nat'l. Lab
Robin S. McDowell
Los Alamos Nat'l. Lab
Larry Cramer
Spectra-Physics Inc.
William C. Stwalley
University of Iowa
Paul Kleiber
University of Iowa

ICALEO '83 Organizing Committee

GENERAL CHAIRMAN — Sidney S. Charschan
Western Electric, Princeton, NJ

PROGRAM CHAIRMAN — Raymond E. Jaeger
SpecTran Corp., Sturbridge, MA

PROFESSIONAL ADVANCEMENT COURSES
James T. Luxon
General Motors Institute, Flint, MI

TREASURER — James F. Smith
IBM, Research Triangle Park, NC

PUBLIC RELATIONS — William H. Shiner
Laser Inc., Sturbridge, MA

INTERSOCIETY LIAISON — David A. Belforte
Belforte Associates, Sturbridge, MA

1983 ICALEO STEERING COMMITTEE

DAVID WHITEHOUSE
Raytheon Corporation, Chairman

JACK ALDRIDGE
Los Alamos National Laboratory

DAVID BELFORTE
Belforte Associates

SIDNEY CHARSCHAN
Western Electric Engineering Center

DAVID EDMUNDS
Xerox Corporation

JAMES LUXON
General Motors Institute

JAMES F. SMITH
IBM Corporation

Contents

	Page
<u>FUNDAMENTALS OF LASER PROCESSING</u>	
Laser-Plasma X-Ray Source for X-Ray Lithography H M Epstein	1
A New Preionization Technique for High Repetition Rate Pulsed Gaseous Lasers R Marchetti, E Penco, and G Salvetti	10
Beam Profile Measurement of High Power CO ₂ Laser M Ikeda, A Yamada, and K Shinohara	16
A C-Radius Technique for Determination of Beam Profiles D U Chang	22
Focusing and Depth of Focus of Gaussian and Higher Order Mode Beams J T Luxon	31
CO ₂ Laser Dryer for Offset Rotary Press M Ikeda, H Kawasumi, and T Arai	37
The Influence of a Plasma During Laser Welding, R D Dixon and G K Lewis	44
Plasma Plume Effects in Pulsed CO ₂ Laser Spot Welding R S Arnot and C E Albright	51
<u>LASER WELDING</u>	
Beam Hole Behaviour During Laser Beam Welding Y Arata, N Abe, and T Oda	59
Porosity Decrease in Laser Welds of Stainless Steel Using Plasma Control W B Estill, and B D Formisano	67
CO ₂ Laser Welding of Deep Drawing Steel Sheet and Microalloyed Steel Plate C J Dawes and M N Watson	73
HSLA Steel Laser Beam Weldments P E Denney, and E A Metzbower	80
Results of Underwater Welding with High Power CO ₂ Lasers G Sepold, and K Teske	87
Laser Welding in High Production C Kymal	90

	Page
<u>SURFACE MODIFICATION</u>	
Condition Setting Method Utilizing Data Base System in CO ₂ Laser Surface Hardening Y Arata, K Inoue, and S Matsumura	100
Effects of Process Parameters on Laser Surface Modification C A Liu, and M J Humphries	108
Laser Transformation Hardening of a Medium Carbon Steel P J Oakley	118
Surface Hardening of Titanium by Laser Nitriding S Katayama, A Matsunawa, A Morimoto, S Ishimoto, and Y Arata	126
Ceramic Coating with High Power CO ₂ Laser M Ikeda, S Mineta, N Yasunaga, and S Fujino	134
The Importance of the Laser Welding Technique in Prosthetic Dentistry H van Benthem, and J Vahl	140
Flexible Beam Delivery for Material Processing Laser Power through a Fiber Optic Cable M G Jones and G Georgalas	148
<u>CUTTING AND DRILLING</u>	
Comparison of Metal Removal by Alexandrite and Nd:Yag Laser Beams J T Puglis and J Gomba	153
Laser Beam Cutting of Thick Steel G Sepold and R Rothe	155
A Quantitative Theory for the Role of Oxygen in the Laser Cutting Process M Lepore, M Dell'Erba, C Esposito, G Daurelio, and A Cingolani	159
Laser Adjustment of Linear Monolithic Circuits A Litwin and D V Smart	165
Development of a Multi-Workstation Laser Processing Facility F B Hardisty	173
Laser Reflow Soldering of Film Capacitors W J Fanning	179
The Design of a CNC Laser Drilling Machine for the Production of High Quality Holes in Aerospace Components T M Weedon	190

	Page
<u>COMPUTER MODELING</u>	
Basic Analysis of Metal Removal Neodymium Lasers M G Jones and G Georgalas	197
A Three Dimensional Heat Flow Model for Prediction of Case Depth in Laser Surface Transformation Hardening O A Sandven	206
Numerical Modeling of Laser Material Processing S Rajaram, and R J Coyle	214
Absorption Measurements for High Power Material Processing P Gay and G Manassero	222

Laser-plasma x-ray source for x-ray lithography

Harold M. Epstein

Electronics Department, Battelle's Columbus Laboratories
505 King Avenue, Columbus, Ohio 43201

Abstract

Laser-plasma x-ray sources have been evaluated for submicron x-ray lithography. Exposure machines based on available, repetitively pulsed lasers of reasonable cost appear to be attractive. These machines would make full wafer exposure levels in times consistent with present manufacturing requirements.

Introduction

X-ray lithography is a logical extension of the near contact optical and U.V. printing techniques into the soft (0.25 - 3.0 keV) x-ray regime.^{1,2} The technology has advanced to the point where submicrometer line width patterns can be produced with a throughput of more than one 75 mm diameter wafer level per minute. An x-ray exposure machine with these capabilities, using a Pd-La anode in a 4.5 kW electron beam x-ray unit, was developed at Bell Laboratories.^{3,4}

Although electron beam x-ray sources may be satisfactory for the first generation of machines, future developments will almost certainly depend on the higher brightness, non-conventional x-ray sources such as pulsed plasmas.⁵⁻¹⁰ Conventional production of line width patterns significantly smaller than 1 micrometer requires combinations of softer x-rays, smaller source diameter, and higher time average x-ray power and brightness that are difficult to achieve with electron beam x-ray source.

This paper discusses the optimization of high pulse rate laser-plasma x-ray sources for submicrometer x-ray lithography. Because it is not possible to optimize the x-ray source isolated from the other components of the x-ray lithography exposure machine, such topics as windows, masks, and photoresist will also be discussed. In many situations, the applicable materials research is not available to adequately match the source to a systems component such as the photoresist or mask. When these situations occur, the optimization will be based on the present component status, but an evaluation of the benefits from expected improvements will be included.

The general advantage of the high pulse rate laser-plasma x-ray source over conventional electron beam x-rays are: (1) the small source diameter drastically reduces the penumbra effect and allows short source-mask distances for step and repeat exposures²; (2) the small source diameter allows the x-rays to be extracted from the vacuum through a set of differentially pumped orifices eliminating the need for windows; (3) the x-ray absorption cross-sections of most photoresist components are much higher for the soft x-rays providing greater energy absorption; (4) the photon statistics per unit of absorbed energy in the photoresist is better; and (5) for a given absorber thickness on the mask, the contrast ratio between transmitted and absorbed areas in the pattern is greater for soft x-rays. In addition to these tangible advantages, several other factors favor the laser-plasma x-ray system. Laser technology is relatively new and growing at a rapid rate, so that order of magnitude improvements in average power can be expected in the near future, whereas the electron beam x-ray machine is a rather stable technology. Also, a laser system can be installed outside of a clean room with the beam brought in through an enclosed pipe, saving expensive clean-room space.

Laser-plasma phenomenology

During the optimization process, it is necessary to relate trade-offs between spectral characteristics, efficiency, and laser characteristics. Thus, the physical mechanism that converts the laser light into x-rays is of interest. Briefly, a specially tailored leading edge of the focused laser pulse vaporizes and ionizes the surface of the target creating a low temperature plasma. The plasma that is created absorbs a large fraction of the remainder of the laser pulse and is heated to a temperature slightly below 1 keV (1.2×10^7 K) at a typical laser radiation intensity of 10^{14} w/cm², as seen in Figure 1. X-rays are produced in this high temperature plasma by bremsstrahlung, recombination radiation, and line radiation, all of which originate from electron-ion collisions.¹¹

Unless specified otherwise, the reference system consists of 1.06 μ m neodymium laser light incident on a copper target at an intensity of 10^{14} watts/cm². The x-ray spectrum

8650175

generated with a copper target has a large number of intense spectral lines in a spectral band centered at approximately 1.2 keV (Figure 2). The spectral lines are L-lines emitted from highly ionized species of copper. The band of lines can be moved up or down in energy with targets of higher or lower atomic number. However, Figure 3, which plots conversion efficiency versus atomic number Z , shows copper ($Z = 29$) to be the optimum element for converting neodymium laser light into x-rays above $h\nu \approx 1$ keV, assuming an incident intensity of 10^{14} watts/cm².

The spectral lines are emitted from a plasma layer of electron temperature $T_e \sim 1$ keV and electron density $n_e \sim 10^{21}$ cm⁻³ located near the leading edge of a thermal diffusion front that advances through the low temperature plasma during the lifetime of the laser pulse. To understand the reason for the peaks in Figure 3, it is helpful to realize that the L-lines are mostly caused by inelastic collisions between free electrons and ground state ions. The collisions excite bound electrons from the L-shell to the M-shell, and the x-rays are produced by the spontaneous radiative decay of M-shell electrons back to the L-shell. Targets with Z above the copper peak have energy gaps between the L and M subshells that are too wide to be efficiently excited. Targets with Z below the peak have the problem that the various energy gaps between L and M subshells increasingly fall below 1 keV as Z decreases. These very soft x-rays are unable to penetrate any practical mask substrate and for present purpose need not be considered. Also, the depletion of L-shell populations below the peak causes a decrease in conversion efficiency. The peak in K-shell conversion efficiency at a Z of about 13 can be explained in terms of the K and L subshells in a similar manner. The K-shell peak is much lower in conversion efficiency, but the x-ray emissions are more energetic. An Al target emits predominantly He-like Al K α line radiation at 1.6 keV. The K-peak efficiency can be increased substantially by using shorter wavelength laser light which penetrates to a denser portion of the plasma. However, most of the radiation is continuous recombination radiation with a low energy cutoff at 1.6 keV.

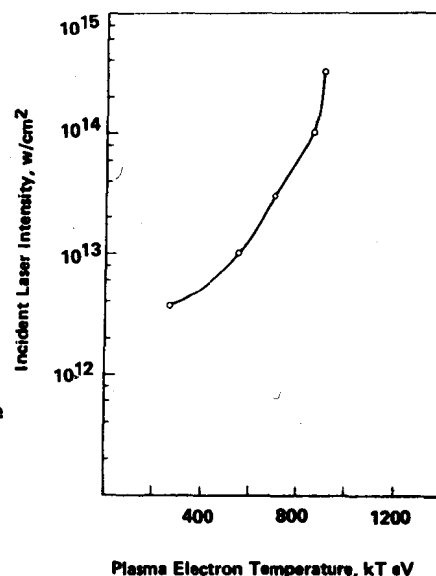


Figure 1. Radiating plasma temperature versus incident laser intensity for Cu targets

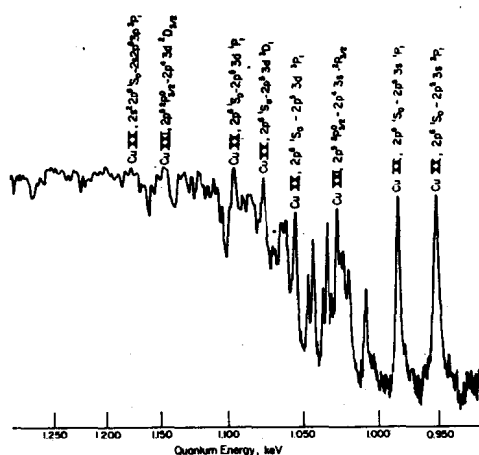


Figure 2. Densitometer tracing of bent crystal spectrograph of x-ray produced from copper target with neodymium laser pulse

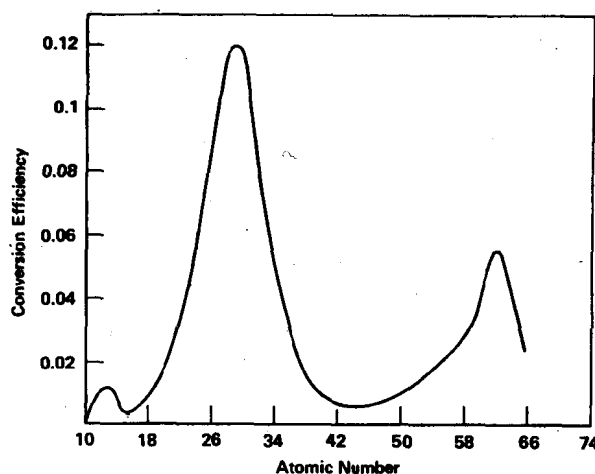


Figure 3. Dependence of x-ray conversion efficiency above 1 keV on atomic number for $1.06 \mu\text{m}$, 10^{14} W/cm²

X-ray interactions

In the x-ray energy range of importance to microlithography, the dominant x-ray interaction mechanism is photoelectron emission. Scattering is negligible, so that x-rays travel in essentially straight lines until captured. Fluorescent yields are also very small for low energy x-rays (less than a few percent) so for all practical purposes, the x-ray energy is converted into electron energy at the first interaction. Normally, the excited atom

returns to the ground state by emission of Auger electrons. The photoelectron and the Auger electrons expose the photoresist. The range of these electrons and diffraction of x-rays at the mask determine the limit of resolution for an ideal x-ray source.¹²

The cross section for capture of the x-ray by electrons varies with the photon wavelength and exhibits large jumps at critical wavelengths or edges. Between the edges, the cross section increases roughly as the cube of wavelength.

In the evaluation of the various components of an x-ray lithography exposure machine, it is necessary to evaluate the attenuation of the x-ray beam through a component. For a monoenergetic x-ray beam, the attenuation I/I_0 is given by

$$I/I_0 = e^{-\alpha(E)x}$$

where I_0 is the incident flux in J/cm^2 , α is the absorption cross section at energy E and x is the attenuation thickness. A more complex spectrum can be divided into energy bands and treated numerically. However, the general exponential shape of the laser-plasma x-ray envelope permits a shortcut for optimization calculations. The three radiation processes have the same statistical exponential spectral dependence for an optically thin plasma of thermal energy (kT) in keV. For a collimated source,

$$I/I_0 = \int_0^\infty \exp [(-\alpha x - h\nu/(kT))] d(h\nu)$$

where $(h\nu)$ is the photon energy (keV). For a material with no edges near 1 keV, $\alpha \approx C_1 (h\nu)^{-3}$, where C_1 is the absorption cross section for the material at 1 keV.

The x-rays emitted from the plasma fall off exponentially with increasing energy, while the x-ray transmissivity of the absorber, $T(h\nu)$ is controlled by the photoelectric absorption cross section and falls off rapidly with decreasing energy. The transmitted x-rays fall in a narrow band as shown in Figure 4. The peak energy of this transmission band, $(h\nu)_m$, is given by

$$(h\nu)_m = 1.32 C_1^{1/4} x^{1/4} (kT)^{1/4} \quad (1)$$

Because of the sharply peaked integral, when kT is less than $(h\nu)_m$, the integral can be evaluated by expanding in a Taylor series about $(h\nu)_m$ (saddle point method), giving

$$I/I_0 \approx 1.5 (kT)^{5/8} x^{1/8} C_1^{1/8} \exp [-1.75 C_1^{1/4} x^{1/4} (kT)^{-3/4}] \quad (2)$$

Now, if we consider a photoresist without absorption edges in the region of $(h\nu)_m$, the absorbed dose, $D(J/cm^2)$ at the surface is given by

$$D \approx .69 (kT)^{-1/8} x^{-5/8} C_1^{-5/8} C_2 I_0 \exp [-1.75 C_1^{1/4} x^{1/4} (kT)^{-3/4}] \quad (3)$$

where C_2 is the absorption coefficient of the resist at 1 keV. If the exponent is less than ~ 1 , the approximation fails.

Resolution

Lack of sharpness in the image of the mask pattern can result from several sources. The primary geometrical effects are the following:

- (1) Source size - the replication error, δ , due to penumbra effects of source size is $\delta = DL/R$. The symbols are defined in Figure 5. This error is decreased when a high λ photoresist is used. The source size becomes a particular problem for step and repeat exposures where R is small. Laser x-ray sources which are about 1/100 the size of conventional sources essentially eliminate this error.
- (2) Wafer warpage - warpage causes a shift and distortion of the pattern projected on the wafer. The warpage replication error δ_w is $\delta_w = w \tan \theta$ where w is the displacement due to warpage (Figure 6). Warpage can be minimized by vacuum back plates to hold the wafer and by use of step and repeat exposures which effectively reduce all dimensions.

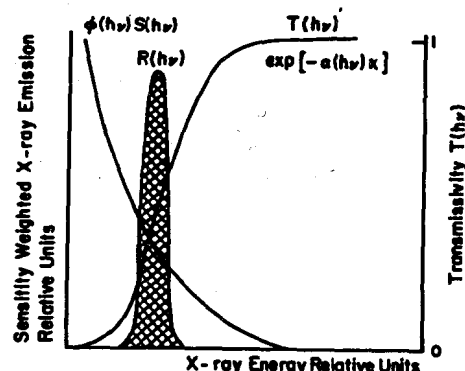


Figure 4. Sensitivity weighted x-rays on photoresist

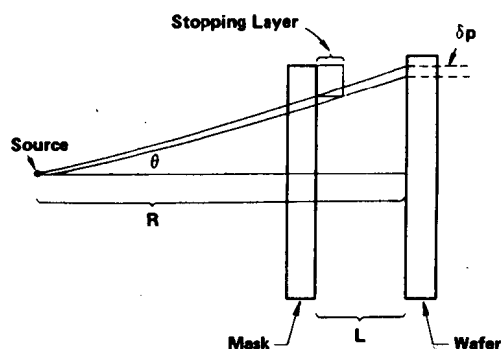


Figure 5. Replication error due to source size

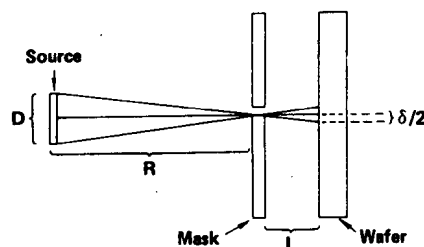


Figure 6. Alignment error due to warpage

- (3) Finite opaque layer penumbra - the thin absorbing layer that forms the pattern on the mask causes an "unsharpness" in the image projected on the wafer (Figure 7). The replication error due to this effect depends on the absorption coefficient of the stopping layer and on the gamma of the photoresist. Assuming that a contrast factor of ten is needed for a good image, this pattern thickness unsharpness δ_p is given by

$$\delta_p = \frac{2.3 \tan \theta}{\alpha_p}$$

The absorption cross section of the pattern layer is very high for the soft x-rays emitted by laser-plasma sources. Thus, δ_p is minimized.

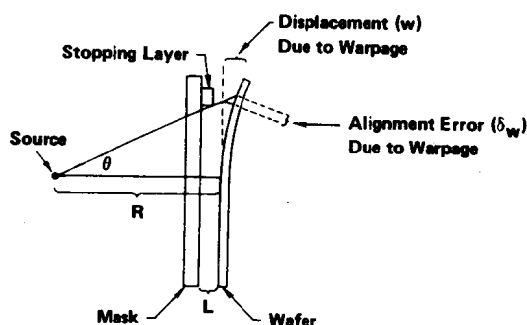


Figure 7. Replication error due to finite thickness of stopping layer

- (4) Fresnel diffraction - there is a replication error, δ_F , due to Fresnel diffraction. Since $R \gg L$, this error is proportional to $\sqrt{\lambda L}$ with a proportionality constant on the order of 1. A diffraction error of 0.1 to 0.2 micrometers can be expected for the mask wafer spacings currently considered.
- (5) Mask alignment - a replication error due to mask alignment is independent of the x-ray source, provided that the source does not impose physical constraints on the alignment system.

In addition, there are several potential sources of unsharpness which are not related to geometry.

- (1) Range of emitted electrons - this effect is very small for soft x-rays¹² of the order of 5 to 65 nm.
- (2) Finite size of photoresist molecules - the effective resolution cannot be better than the diameter of the resist molecules.
- (3) Photon statistics - if the exposure is to avoid a statistical mottle, it is necessary to have many photons absorbed in each resolution element. Statistically, 1/e of the elements will have an exposure variance greater than $\sqrt{N/N}$, where N is the average number of absorptions in each element. In most photoresists, the exposure sensitivity is so low that photon statistics is not a limiting factor.

Basic lithographic exposure system

The basic configuration used in generating x-rays for lithography is shown in Figure 8. In our reference system, 1.06 micrometer wavelength laser pulses with an energy of 0.3 joules and a pulse width of 0.2 nanoseconds are focused onto a copper target to a spot size of about 40 μm . Approximately 25 percent of the incident light is converted into x-rays in the 0.3 to several keV range. Approximately 10 of the 25 percent lies between 1 and 2 keV.

The target is a relatively large cylinder that advances on a helical drive to present a fresh, nearly flat surface area to successive laser pulses. Since each laser pulse destroys only about 10^{-4} cm² of target area, a cylinder with 100 cm² of surface area will give about a million x-ray pulses.

A mask/wafer assembly (Figure 8b) is placed 5 cm from the source. This distance maintains δ_p less than 0.1 micrometer and allows a reasonable number of step and repeat exposures for the wafer. The x-ray outputs which we cited refer to x-rays emitted into the 2π steradians facing the mask/wafer assembly.

The small source diameter permits a solution to the troublesome problem of designing an x-ray window to bring the soft x-rays out of the vacuum and into an atmospheric pressure helium expansion chamber. Figure 8 shows the x-rays directed out of the vacuum chamber through a set of differentially pumped orifices. The first hole has a diameter of ~ 1 mm and is located less than 2 mm from the source, so that all of the x-rays directed at the desired portion of the mask will pass through the holes.

Laser parameters

For the high-average power required in x-ray lithography, it is advantageous to use a low pulse energy, high repetition rate laser. It can be seen from Figures 3 and 9 that the preferred target intensity is $\sim 10^{14}$ watts/cm² for 1.06 μ m laser light. Conversion efficiencies and temperatures fall off rapidly as intensities fall below this level, while intensities much greater than 10^{14} lead to extra costs and to complications worth avoiding. The conversion efficiency depends on several other parameters besides peak intensity. Since the critical density boundary is moving during the pulse, it is desirable to have the focusing cone angle as small as possible to maintain the focal intensity. On the other hand, a high f number system yields a large focal spot for a given beam divergence Δ , and diameter D_b . The optimum f number of the lens, f_{opt} , is given by

$$f_{opt} \sim \left(\frac{v\tau}{D_b \Delta} \right)^{1/2} \quad (3)$$

where v is the velocity of the critical intensity boundary and τ is the laser pulse width (FWHM). For a Cu target under conditions of interest, $v \sim 3 \times 10^7$ cm/sec.¹¹ To exceed the 10^{14} w/cm² peak focused intensity with an optimum lens and a Cu target, the laser energy, E_L , should meet the following conditions:

$$E_L > 10^{14} \tau^2 D_b v \Delta \quad (4)$$

Wave length is not considered in this scaling relationship, but for a Cu target, no significant difference in conversion efficiency or temperature was observed when the irradiation wavelength was changed from 1.06 to 0.53 μ m. For elements whose primary x-ray emissions are from the K-shell, efficiencies are appreciably improved at shorter wavelengths.

Some care must be exercised in using this scaling relationship for pulse widths appreciably below 10^{-9} seconds. The difficulty is that the plasma radiates most of the x-rays at an electron density near $n_e \sim 10^{21}$ cm⁻³, so that the characteristic time required for the radiating ions to strip down to a quasi-steady degree of ionization is approximately $10^{12}/n_e \sim 10^{-9}$ seconds.¹³ However, only a thin layer of matter in the plasma is radiating x-rays significantly at any given time during the pulse, and the time that is spent in the critical zone is a small fraction of a nanosecond. The phenomenological description of the layers that successively radiate the x-rays is the same for pulse widths down to about 0.1 nanosecond.

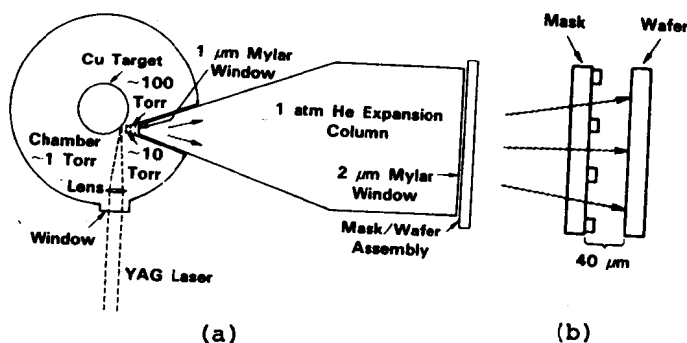


Figure 8. Experimental configuration with differentially pumped orifices

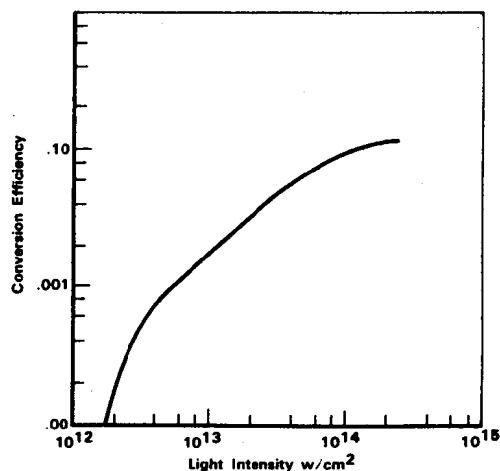


Figure 9. Conversion efficiency to x-rays above 1 keV for 1.06 μ m laser light

We are now in a position to discuss the selection of a candidate laser. The highest average power laser available as a commercial laser which meets the criteria of Equation 4 is the Quantel 402 DP with a pulse rate of 10 Hz, a pulse width of 0.2 nanoseconds and a pulse energy of .3 Joule. At the 10 percent conversion efficiency, this would yield 0.3 watts of x-ray power. The cost of this system is approximately \$100,000. Several systems under development promise to provide higher average powers within a few years and still meet the criterion of Equation 4. The multiple reflection slab laser system under development¹⁴ promises average powers up to 1 Kw. Also, development of reinforced glass rods to permit an order of magnitude increase in average pumping rates could lead to a relatively inexpensive glass rods system with an average power in the tens of watts in the near future.¹⁵ Longer range possibilities include gas lasers such as the Eximers and Iodine.

Mask/Substrate

A major limitation in submicron lithography is the thickness of the absorber mask required to produce an adequate contrast. Most masks are fabricated with electron beam lithography. Since scattering of electrons makes the production of deep vertical walls difficult, the aspect ratio achievable in the mask is one limitation to x-ray lithography. It is instructive to compare the thickness of Au and U-238 required to produce a factor of ten dose contrast in the photoresist with laser-plasma x-rays (kT = .85 keV) and Pd-La x-rays (2.84 keV). For the laser plasma system, the resist will be considered to be undoped and composed of low atomic number elements. The dose contrast is independent of the resist and substrate for the nearly monoenergetic Pd-La system, and a gold layer of 0.49 μm is needed.

The thickness of Au required on the 4 mm Si substrate for a laser plasma source is less than half that for the Pd-La. The difference is even larger for U-238. We have used 4 μm and 3 μm thick Si substrates for laser plasma lithography. Reference 16 discusses 2.5 μm SiC mask substrates. The advantages of thin substrates for high contrast are evident from Table 1. The largest part of the attenuation through the uncoated substrate comes from the removal of the very soft component of x-rays (less than 1 keV) which were not included in the 10 percent conversion efficiency.

Table 1. Mask contrasts and attenuations and PMMA energy deposition (plasma temperature .85 keV)

x_{Si} nm	Equivalent x_{SiC} μm	For contrast of 10 x_{Au}	For contrast of 10 $x_{\text{U-238}}$	Substrate Attenuation	D/I ₀ PMMA cm^{-1}
2	1.30	.12	.10	.21	320
4	2.61	.19	.16	.16	150
6	1.95	.27	.23	.13	88
8	5.21	.34	.28	.12	66

Photoresist

Most of the photoresists used in lithography are polymers. Resists are classified as positive or negative depending on whether their solubilities in the developer are enhanced or diminished by irradiation. When a long chain polymer is subjected to ionizing irradiation, valence bonds are broken causing the solubility of the resist in the developer to change. Since most of the bond breakage is caused by secondary electrons in either electron or x-ray exposures, the sensitivity of the resist in terms of volumetric energy absorption is not dependent on the type of radiation to a first approximation. With x-rays, the absorptions occur preferentially in the higher atomic number atoms, but the photo-electric event is in a deep subshell and the range of the Auger electrons is much greater than atomic distances.

As can be seen from Equation 3, the volumetric energy deposition rate in the resist is proportional to C_2 , the x-ray cross section at 1 keV (assuming no absorption edges within the sensitivity peak, and a thin mask substrate). Doping a resist with heavy elements to increase the absorption cross section is an effective method for increasing the efficiency of resists to soft x-ray. Substituting a Th atom for one C or H atom in each methyl methacrylate unit in PMMA increases the absorption by a factor of 4.

The size of the polymer molecule in a resist plays a similar role to the size of a grain in photographic emulsions. If the number of chain scissions required to expose a molecule were independent of the molecule size, the exposure sensitivity would be proportional to

the molecule's volume or the solubility would be approximately proportional to the molecular weight.

Finally, the sensitivity can be altered by changing the chemical structure of the polymer. A Soviet study of the effect of chemical structure and distribution of carboxyl groups in resist materials exposed to laser-plasma x-rays showed very promising results.¹⁷ The sensitivities of copolymer methylmethacrylate and methacrylic acid resists were improved to the extent that they were fully exposed by two laser-plasma x-ray pulses at a distance of 10 cm. The x-ray yield per pulse was 400 mj between 1.5 and 15 Å and the film was covered by 3 µm of Laysan coated with 0.3 µm Al. Under these conditions, the resist exposure was under 1 mj/cm². This is comparable to the sensitivity of the chlorinated photoresist developed by Bell Laboratories for Pd-La x-ray exposures.¹⁸

The gamma curve for resists is usually defined as

$$\gamma = [\log D^{1.0}/D^i]^{-1}$$

where D^i is the initiation dose and $D^{1.0}$ is the dose for 100 percent film removal based on extrapolation of the slope at $D^{0.5}$ (see Figure 10). The γ for a resist is analogous to γ for photographic film and indicates contrast. High γ 's give sharp lines.

System configuration and exposure time

We are now ready to fully specify a system, which can be constructed with essentially current technology as shown in Table 2. While higher average power lasers should soon be developed, a reasonable exposure machine can be based on the commercially available laser listed. The copper target is the best L-shell emitter. While the optimum K-shell emitter gives harder x-rays and lower mask substrate attenuation, the poor conversion efficiency and lower resist absorption make this a poor choice. If resists were to be developed with absorption edges slightly above 1.6 keV, Al might be a good target choice. However, the mask contrast would be poorer. Si is almost optimum as a mask substrate because the laser plasma x-rays fall into the notch below the Si K-edge. However, SiC is not much more absorbing and is transparent to light for interferometry alignment. The target/mask distance of 5 cm is enough to keep the source penumbra "unsharpness" below 0.1 µm, and the step and repeat area of 4 cm² maintains an exposure uniformity better than 5 percent. The 40 µm mask/wafer distance is chosen to correspond to industry practice.³ The choice of photoresist is not clear because of the lack of published data in the x-ray energy range of interest. However, statistics alone would require an energy deposition of ~ 10 J/cm³ for 0.1 µm resolution. If the exposure through the resist is to be held uniform to 10 percent, no more than 0.1 of the x-rays can be captured in the resist, and the highest sensitivity achievable with a 0.5 µm resist thickness (maintaining 0.1 µm resolutions) is ~ 5 mj/cm².

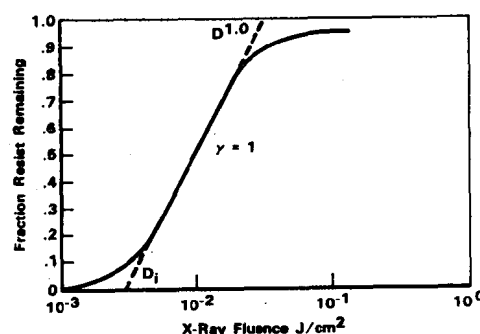


Figure 10. Hypothetical thickness after exposure for negative resist

Table 2. System Parameters

Laser	Quantel 402 DP .3 J/pulse, 10 Hz, $\tau = .2$ nsec, $\lambda = 1.06$ µm, $D_p = .95$ cm, $\Delta = 7 \times 10^{-4}$ rad
Lens	3 cm focal length
Target	Copper cylinder
Window	Differentially pumped orifices
Mask substrate	2.5 µm SiC
Mask Absorber	.2 µm Au
Target/mask distance	5 cm
Mask/wafer distances	40 µm
Exposure system	Step and repeat
Step exposure area	4 cm ² , 2 cm x 2 cm
Resist	Sensitized, doped copolymer

Assuming a resist with a sensitivity of 5 mJ/cm² and the system of Table 2, the exposure time for each step is 6.5 seconds, giving a throughput of 1.6 cm²/sec, neglecting repositioning time.

Conclusions

The laser-plasma x-ray source has a very high average brightness, only about a factor of ten lower than the Spear synchrotron at 1 keV. However, the high brightness achieves its maximum advantage only when the resolution is limited by the source penumbra. Thus, the laser-plasma source compares best with conventional sources for high resolution applications. It should be expected that as IC demands require resolution of 0.1 μ m or better that this type of source will be increasingly beneficial.

Additional improvements in the average power of commercial high brightness lasers as well as new developments in soft x-ray resists should also make the laser-plasma x-rays source useful for lithography in the μ m range.

References

- (1) H. I. Smith, D. L. Spears, and S. E. Bernacki, *J. Vac. Sci. Technol.*, **10**, 913 (November-December, 1973).
- (2) N. D. Wittels, *Fine Line Lithography*, Chapter 1, R. Newman, ed., North-Holland (1980).
- (3) A. Zacharias, *Solid State Tech.*, 57-59 (August, 1981).
- (4) J. R. Maldonado, M. E. Poulsen, T. E. Saunders, F. Vratny, and A. Zacharias, *J. Vac. Sci. Technol.*, **16**, 1942 (November-December, 1979).
- (5) H. M. Epstein, P. J. Mallozzi, and B. E. Campbell, *SPIE*, **385**, 141 (1983).
- (6) P. J. Mallozzi, H. M. Epstein, and R. E. Schwerzel, *In Adv. in X-Ray Analysis*, G. J. McCarthy et al, Eds., **22**, 267 (1979).
- (7) D. J. Nagel, *Annals N.Y. Acad. Sci.*, **342**, 235 (June, 1980).
- (8) D. J. Nagel, M. C. Peckerar, R. R. Whitlock, J. R. Greig, and R. E. Pechacek, *Electronics Lett.*, **14**, 781 (1978).
- (9) H. M. Epstein, R. L. Schwerzel, and B. E. Campbell, 6th International Workshop on Laser Interactions and Related Plasma Phenomena, eds., G. H. Miley and H. H. Hora, Plenum (1983).
- (10) R. McCorkle, J. Angilello, G. Coleman, R. Feder, and S. J. La Placa, *Science*, **205**, 401 (1979).
- (11) P. L. Mallozzi, H. M. Epstein, R. G. Jung, D. C. Applebaum, B. P. Fairand, and W. J. Gallagher, *Fundamental and Applied Laser Physics: Proceedings of the Esfahan Symposium*, M. S. Feld, A. Javan, and N. A. Warnick, eds., John Wiley & Sons, Inc. (1973).
- (12) E. Spiller and R. Feder, *X-Ray Lithography*, Chapter 3, H. J. Queisser, e., Springer-Verlag (1977).
- (13) R.W.P. McWhirter, *Plasma Diagnostic Techniques*, Chapter 5, R. H. Huddleston and S. L. Leonard, eds., Academic Press, New York, New York (1965).
- (14) J. M. Eggleston, L. J. Kane, J. Outeruchrer, and R. L. Byer, *Opt. Lett.* **7**, 405 (1982).
- (15) J. D. Myers, Kigre, Inc., private communications.
- (16) R. K. Watts, *Solid State Techn.*, 68-71 and 82 (May, 1979).
- (17) V. A. Boiko, A. Ya Vainer, K. M. Dyumaev, S. A. Kireeva, V. F. Limanova, I. Ya Skobelev, A. Ya Faenov, and S. Ya Khakhalin, *Sov. Phys. Tech. Phys.*, **27** (11) (November, 1982).
- (18) G. N. Taylor and T. M. Wolf, *J. Electrochem. Sci.*, **127**, 2665 (December, 1980).

Meet the author

Dr. Epstein is a Senior Research Scientist at Battelle's Columbus Laboratories. He received a B.S. in Physics from the University of Colorado in 1950 and a Ph.D. from The Ohio State University in 1962. He has six patents and an IR-100 award in the field of laser-plasma x-rays.